AD-A114 074 NAVAL COASTAL SYSTEMS CENTER PANAMA CITY FL F/G 17/7
A BALANCED ACTIVE ANTENNA AND IMPULSE NOISE BLANKER SYSTEM FOR --ETC(U)
FEB 82 B R LUDLUM
UNCLASSIFIED NCSC-TM-340-82 SBI-AD-F200 023 NL

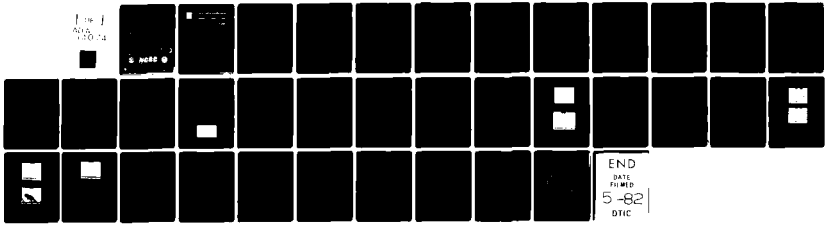

END
DATE FILMED
5-82
DTIC

TECHNICAL
MEMORANDUM
NCSC TM 340-82

FEBRUARY 1982

A BALANCED ACTIVE ANTENNA AND IMPULSE NOISE BLANKER SYSTEM FOR THE RAYDIST T RADIO NAVIGATION RECEIVER

BOBBY R. LUDLUM

NAVAL COASTAL SYSTEMS CENTER
NCSC
PANAMA CITY, FLORIDA 32407

NCSC TM 340-82

[redacted]

NAVAL COASTAL SYSTEMS CENTER

PANAMA CITY, FLORIDA 32407

CAPT RAYMOND D. BENNETT, USN
Commanding Officer

GUY C. DILSWORTH
Technical Director

ADMINISTRATIVE INFORMATION

The work described in this report was done under NAVAIR Project WCSC9.

The author wishes to acknowledge the contributions of John Cowan and Paul Eisenhauer, Code 722, and Otis Stubbs, Code 723.

Released by
R. D. Turnage, Head
Mine Countermeasures Development Division
February 1982

Under authority of
H. H. Lacey, Head
Undersea Countermeasures
Department

UNCLASSIFIED

SECURITY CLASSIFICATION OF THIS PAGE (When Data Entered)

REPORT DOCUMENTATION PAGE		READ INSTRUCTIONS BEFORE COMPLETING FORM
1. REPORT NUMBER NCSC TM 340-82	2. GOVT ACCESSION NO. AD-A114 074	3. RECIPIENT'S CATALOG NUMBER
4. TITLE (and Subtitle) A Balanced Active Antenna and Impulse Noise Blanker System for the Raydist T Radio Navigation Receiver		5. TYPE OF REPORT & PERIOD COVERED 6. PERFORMING ORG. REPORT NUMBER
7. AUTHOR(s) Bobby R. Ludlum		8. CONTRACT OR GRANT NUMBER(s)
9. PERFORMING ORGANIZATION NAME AND ADDRESS Naval Coastal Systems Center Panama City, FL 32407		10. PROGRAM ELEMENT, PROJECT, TASK AREA & WORK UNIT NUMBERS NAVAIR Project W0529
11. CONTROLLING OFFICE NAME AND ADDRESS		12. REPORT DATE February 1982 13. NUMBER OF PAGES 32
14. MONITORING AGENCY NAME & ADDRESS(if different from Controlling Office)		15. SECURITY CLASS. (of this report) UNCLASSIFIED 15a. DECLASSIFICATION/DOWNGRADING SCHEDULE N/A

16. DISTRIBUTION STATEMENT (of this Report)

Approved for public release; distribution unlimited.

17. DISTRIBUTION STATEMENT (of the abstract entered in Block 20, if different from Report)

18. SUPPLEMENTARY NOTES

19. KEY WORDS (Continue on reverse side if necessary and identify by block number)

Navigation Systems; Radion Navigation; Antennas; Towing Cables; Helicopters; Balance; Radio Receivers; Raydist T; Noise Blanker

20. ABSTRACT (Continue on reverse side if necessary and identify by block number)

Erratic operation of Raydist T radio navigation equipment aboard mine countermeasures helicopters has been traced to fuselage-tow cable interactions with the Raydist receiving antenna and to negative-corona generated impulse noise. The development of a balanced active antenna and an impulse noise blanker which have proved successful in reducing these detrimental effects are described. The final system is described in detail and the results of laboratory tests are presented.

DD FORM 1 JAN 73 1473 EDITION OF 1 NOV 65 IS OBSOLETE

S/N 0102-LF-014-6601

UNCLASSIFIED

SECURITY CLASSIFICATION OF THIS PAGE (When Data Entered)

TABLE OF CONTENTS

	Page No.
INTRODUCTION	1
ANTENNA DEVELOPMENT	2
INTRODUCTION	2
Orthogonal Loop Antenna	4
Active Vertical Dipole Antenna	4
Noise Performance	9
Input Impedance	12
Common Mode Signal Rejection	12
Linearity	12
Preamplifier Circuit Description	14
NOISE BLANKER DEVELOPMENT	16
INTRODUCTION	16
NOISE BLANKER SYSTEM CIRCUIT DESCRIPTION	20
Low-Pass Filter	20
High-Pass Filter	20
Power Splitter, Delay Line, and Blanking Switch	25
Noise Pulse Detector and Blanking Pulse Generator	25
Isolation Amplifier	28
CONCLUSIONS	28

LIST OF ILLUSTRATIONS

Figure No.		Page No.
1	Balanced Dipole Antenna and Noise Blanker System for Raydist T	3
2	Orthogonal Ferrite Loaded Loop Antenna	5
3	Vertical Dipole Antenna	7
4	Mast-Mounted Dipole Antenna Equivalent Circuit	8
5	Antenna Equivalent Circuit Seen by Preamplifier	8
6	Equivalent Circuit - Signal and Noise Referred to Input	9
7	Equivalent Circuit (Unbalanced)	10
8	Signal-to-Noise Ratio	11
9	Cross Modulation Performance	13
10	Active Dipole Antenna Preamplifier	15
11	Test Pulse Generator Schematic	16
12	Test Generator Pulse Characteristics	17
13	Basic Impulse Noise Blanker	18
14	Noise Blanker System	19
15	Noise Blanker System Waveforms	21
16	System Output Frequency Spectrum	22
17	Low-Pass Filter (Chebyshev, N = 5, Passband Ripple = 0.01 dB, f_c = 5.5 MHz)	23
18	High-Pass Filter Schematic and Frequency Response	24
19	Power Splitter/Delay Line/Blanking Switch	26
20	Noise Pulse Detector/Blanking Pulse Generator	27
21	Isolation Amplifier	29

INTRODUCTION

An investigation by the Naval Coastal Systems Center (NCSC) and McDonnell Douglas Research Laboratories (MDRL) of erratic behavior of Raydist T radio navigation equipment aboard AMCM helicopters resulted in the discovery of two tow-cable related sources of interference:

1. Interaction between the Raydist receiving antenna (a short vertical monopole) and the helicopter fuselage-tow cable system acting as an end-fed long wire antenna produces large variations in the magnitude and the phase of the received signals.

2. Negative-corona discharge (Trichel pulses) from the cable end produces broadband impulse type noise which is capable of producing nonlinear effects (overload) and oscillatory transient effects (ringing) in the narrow bandwidth receiver circuits. This corona discharge is due to the helicopter fuselage-tow cable system becoming highly negatively charged by ion transport in the turbine engines or by triboelectric effects.

Analytical studies and scale model measurements by MDRL[1] indicated that the use of an electrically balanced receiving antenna, i.e., one which would not depend on the helicopter fuselage as a ground plane or counterpoise, would reduce the first source of interference. The second source of interference, impulse noise, has been dealt with in radio communication systems by the use of a noise blanker which disables the receiver for short periods to prevent the passage of the noise pulses into the narrow bandwidth portions of the system.

The hardware which was designed and built at NCSC to provide a balanced receiving antenna and an impulse noise blanker for the Raydist T receiver is described in this report. The data from field operations in which this equipment was used indicate a marked improvement in the operation of the Raydist T system aboard AMCM helicopters (refer to NCSC Code 720 departmental letter report by Paul Eisenhauer dated January 1982).

---

[1]McDonnell Douglas Report No. MDC Q0688, "Compatibility of the RH-53D Minesweeping Helicopter and Raydist Navigation Set," by J. F. Schaeffer and Medgyeshi-Mitschang, 15 August 1979, UNCLASSIFIED.

The overall system as shown in Figure 1 consists of an electrically very short vertically polarized dipole and preamplifier mounted on a mast on the underside of the helicopter fuselage and an inboard package containing the noise blanker, antenna actuator controller, and power supply. The antenna mast is stowed in a horizontal position for landing and is extended vertically in flight by a motor-driven actuator. A novel feature of the system is that since the noise blanker operates on the low level radio frequency signals from the balanced antenna no internal modifications or connections must be made to the Raydist receiver. The output of the antenna/noise blanker system is a single coaxial cable that connects to the Raydist receiver antenna input connector. Improvements to the Raydist system itself include introduction of the GA-62 position indicator with variable phase-meter damping and monitoring of the automatic gain control (AGC) and phase meter signals using a strip chart recorder as described in Eisenhauer's letter report.

ANTENNA DEVELOPMENT

INTRODUCTION

An ideal receiving antenna for the Raydist T system would have the following characteristics:

1. Responsive to the vertical electric field component or to the horizontal magnetic field component of the propogating electromagnetic wave from the Raydist transmitting antennas.

2. Electrically balanced with respect to the helicopter fuselage-tow cable system such that signals produced by RF currents flowing therein appear as common mode signals and are suppressed by the differential nature of the antenna.

3. Omnidirectional in amplitude response in the horizontal plane.

4. Omnidirectional in phase response in the horizontal plane.

5. Sufficiently sensitive and having sufficient bandwidth to provide adequate signals to the Raydist receiver.

Two types of antennas were built and tested: an orthogonal loop H-field antenna and a short vertical dipole E-field antenna. The loop antenna which ultimately proved inferior to the vertical dipole antenna is described briefly below after which a more detailed description of the vertical dipole is given.

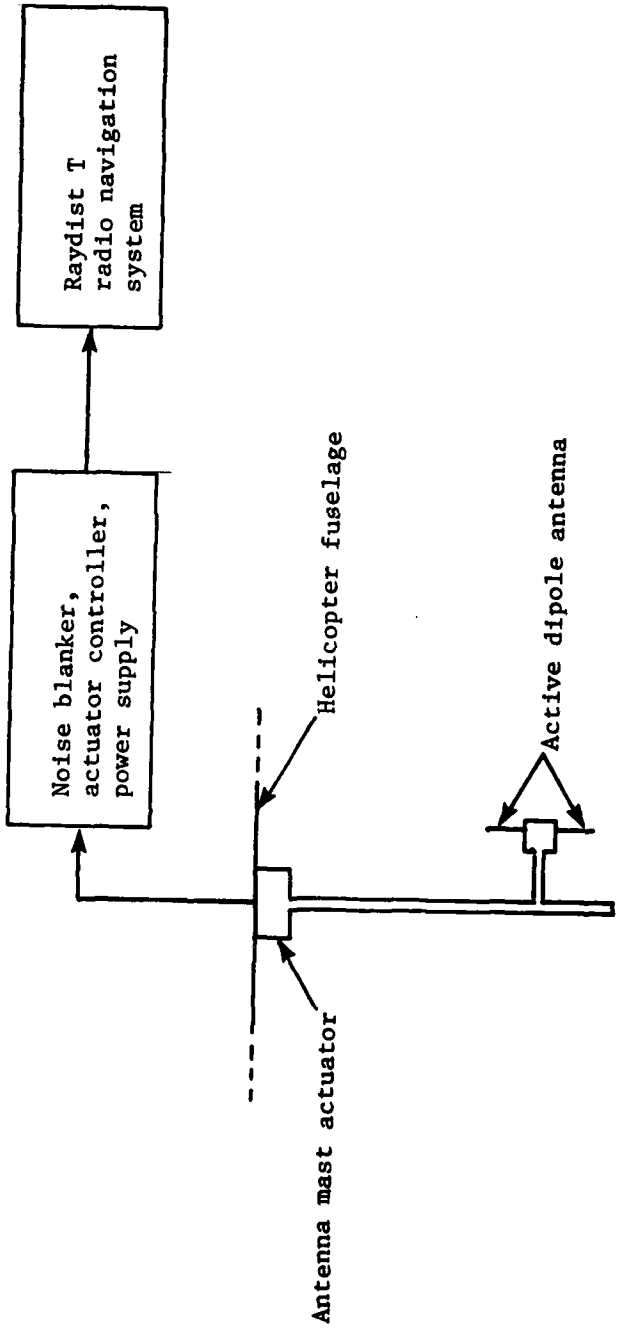

FIGURE 1. BALANCED DIPOLE ANTENNA AND NOISE BLANKER SYSTEM FOR RAYDIST T

Orthogonal Loop Antenna

This antenna (Figure 2) is sensitive to the horizontal magnetic field component and consists of two orthogonal ferrite loaded solenoidal loops and two preamplifiers inside a Faraday shield for electrostatic isolation. The loops are broadly tuned ($Q \tilde{=} 1.4$) to the geometric mean frequency between the Raydist sideband and CW frequencies ($f_c \tilde{=} 2.34$ MHz.). Thus one pair of loops covers the required range of frequencies. The outputs of the two loops are summed in quadrature by a second-order 90-degree all-pass phase difference network and a two-way 0-degree hybrid transformer. The amplitude of the resultant output is omnidirectional. The phase of the resultant output unfortunately is a function of the arrival angle of the received wave and changes by 360 degrees for each complete rotation of the antenna. This produces a phase error which changes with helicopter heading. This problem is solved by adding a corrective phase shift dependent on heading to cancel the phase error due to the antenna. This is accomplished using a quadrature-fed goniometer phase shifter mechanically driven through a servo repeater by the output of a directional gyro. There are additional phase shift errors which are not so easily eliminated. A full Raydist T net consists of four transmitting stations. Generally at a given location within the area covered by the net there will be signals arriving from four different directions and each signal will experience a different phase shift. This produces a distortion of the normally hyperbolic lines of position. A solution to this problem which is probably correctable in software was not attempted.

The antenna was mounted inside a cylindrical plastic housing which exited the air frame through the cargo winch opening and extended about 30 centimetres below the fuselage.

Flight tests with no tow cable showed good receiving characteristics and excellent correction by the gyro/phase shifter. Flight tests with tow cable, however, showed poor cancellation of tow cable effects. This is probably due to the sensitivity of the antenna to magnetic fields caused by fuselage-tow cable currents. An improvement could probably be realized by increasing the separation between the antenna and the fuselage. The attendant mechanical problems coupled with consideration of the problem due to anisotropic phase response and the additional complexity of the gyro and phase shifter resulted in this approach being abandoned in favor of that using the vertical dipole antenna.

Active Vertical Dipole Antenna

This antenna, which is sensitive to the vertical electric field component, consists of a vertically oriented, electrically very short dipole (less than 0.004λ) and a differential, high-input impedance preamplifier mounted at the dipole feedpoint. A single coaxial cable connects the preamplifier to the rest of the system and carries both RF signals and dc power.

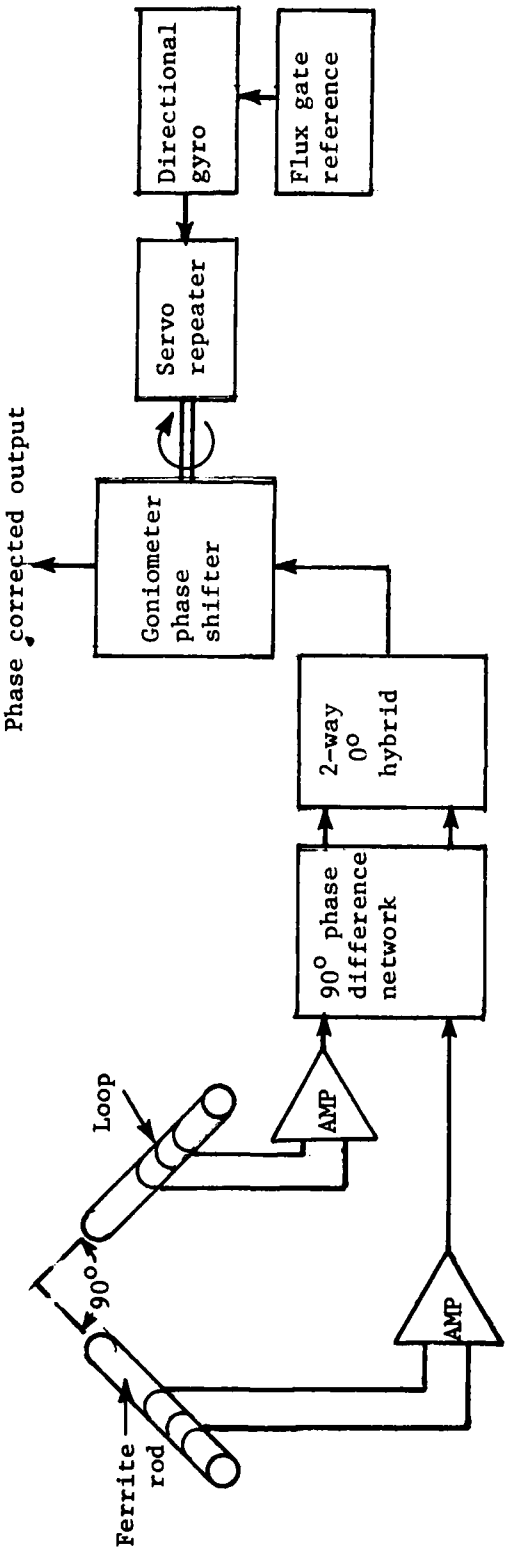

FIGURE 2. ORTHOGONAL FERRITE LOADED LOOP ANTENNA

This type antenna has the potential of meeting all the requirements listed above, but care must be taken to preserve the balance of the antenna by equalizing the coupling between the helicopter-tow cable system and the two halves of the dipole. This is achieved by locating the antenna as far beneath the fuselage as practicable and by keeping the dipole elements as short as practicable. In the present system, the antenna is located about 1.5 metres below the fuselage and the total dipole length is 35 centimetres (Figure 3).

Short vertical antennas are inherently broadband and may be modeled by an ideal voltage source v_i in series with an impedance Z_A.[2] The induced open circuit voltage is given by

$$v_i = h_e E_z \text{ (volts)}$$

where E_z is the vertical electric field intensity in volts per metre and h_e is the antenna's effective height in metres. For vertical antennas with a triangular distribution of current, the effective height is one-half of the actual length of the antenna.[3] The impedance Z_A is given by

$$Z_A = R_R + R_L - j \frac{1}{2\pi f C_A}$$

where R_R is the radiation resistance, R_L is the resistance due to losses, and C_A is the antenna capacitance. For a typical short monopole of height to diameter ratio of about 50, C_A is approximately 11.4 picofarads per metre of length.[2] For short low loss antennas R_R, R_L, and C_A are small so

$$R_R + R_L << \frac{1}{2\pi f C_A} \quad .$$

The antenna equivalent circuit then simplifies to the ideal voltage source v_i in series with the small capacitance C_A. In the following discussion, each half of the vertical dipole is modeled in this manner.

The differential and common mode responses and the capacitance of the dipole antenna were measured at 1.656 MHz with the antenna and support mast vertically oriented above an aluminum screen ground plane. Local vertical electric field intensity was measured with a Stoddart NM-25T field intensity meter. Capacitance values were measured directly with a vector impedance meter and also calculated from measurements of output signal level for different values of preamplifier input capacitance both of which yielded excellent agreement with the approximation given above. Good agreement was found between theoretical and measured values of the effective heights. The total measured equivalent circuit for the mast-mounted

---

[2]Watt, Arthur D., "VLF Radio Engineering, p. 401, Pergamon Press, 1967.

[3]Jasik, Henry (Editor), "Antenna Engineering Handbook," pp. 2-3, 1961.

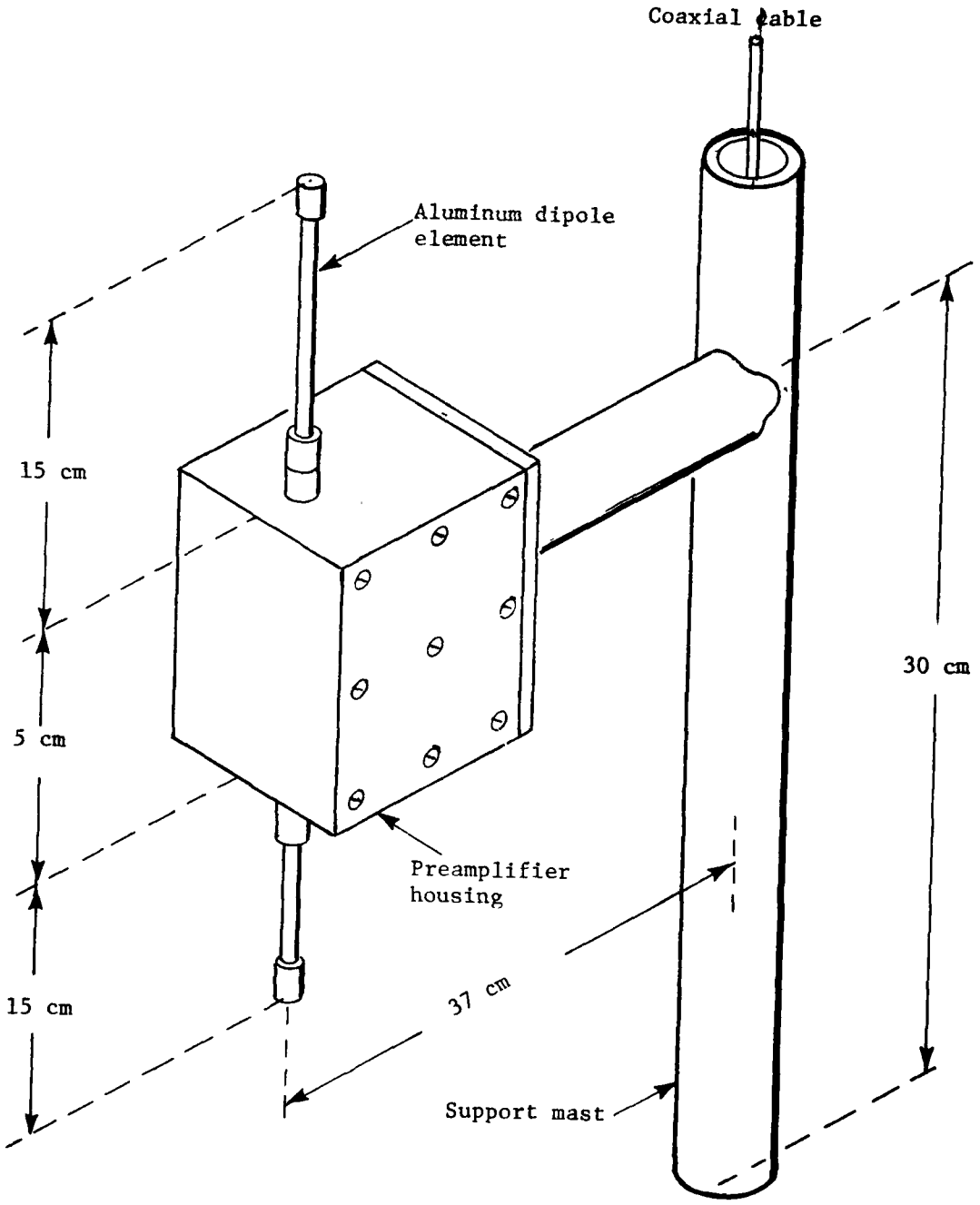

FIGURE 3. VERTICAL DIPOLE ANTENNA

dipole antenna is shown in Figure 4 where v'_{d1} and v'_{d2} represent the differential outputs from the dipole elements and v'_{cm} is the common mode output signal.

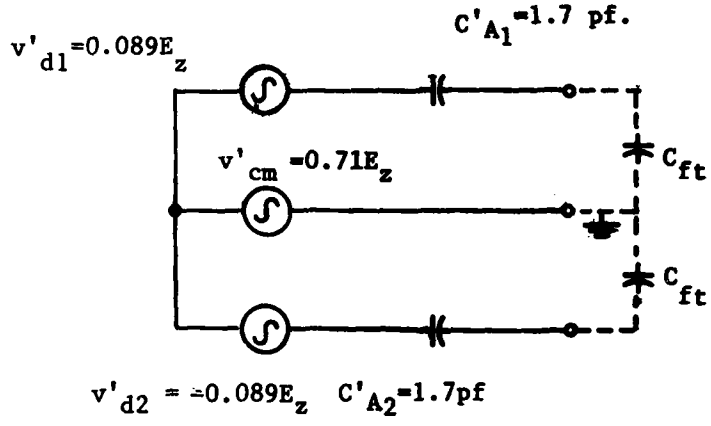

FIGURE 4. MAST-MOUNTED DIPOLE ANTENNA EQUIVALENT CIRCUIT

The capacitance shown by broken lines in Figure 4 represents that of the dipole element feed-through and mounting structure and is about 4.3 picofarads for each element. Including these two capacitors results in the Thevenin equivalent circuit as seen by the preamplifier in Figure 5.

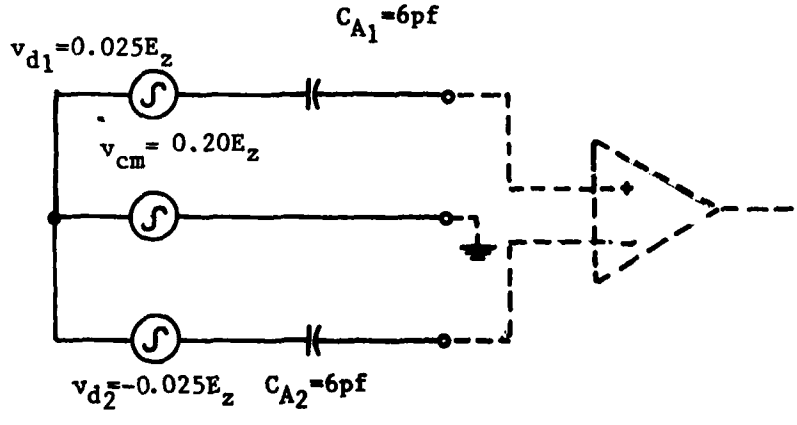

FIGURE 5. ANTENNA EQUIVALENT CIRCUIT SEEN BY PREAMPLIFIER

The signal source characteristics of the short dipole as shown by the equivalent circuit indicate that the preamplifier should have low self-noise, high-impedance differential input, and a high degree of common mode signal rejection. A high degree of linearity over a wide dynamic range is also a desirable feature.

Noise Performance

The output signal-to-noise ratio of an ideal active antenna, i.e., one with integrated passive antenna elements and active amplifying circuits, should be determined by the ratio of desired signal to atmospheric noise. This is accomplished by adjusting the size of the passive elements such that the received atmospheric noise is much larger than the self-noise of the preamplifier. A good compromise between size and noise performance is obtained by choosing a size which equalizes the received atmospheric noise and the self-noise. In the frequency range of 1 MHz to 10 MHz this would require dipole elements about 1 metre long.[4] Such a large dipole antenna could not be used on the helicopter and still be separated from it sufficiently to preserve its balance as discussed above. Therefore, in the present system the noise performance is set by the preamplifier. Satisfactory noise performance of preamplifier (and the rest of the system) was verified by demonstrating that low level Raydist signals were not degraded by passage through the antenna-noise blanker system before entering the Raydist receiver. For this test the signals were fed into the preamplifier through an antenna equivalent circuit network and a comparison was made between the response of the Raydist receiver to direct input signals and the response to signals fed through the antenna-noise blanker system which produced the same test signal levels at the receiver input.

Assuming that common mode signals are suppressed and referring all signal and noise voltages to the input gives the equivalent circuit shown in Figure 6.

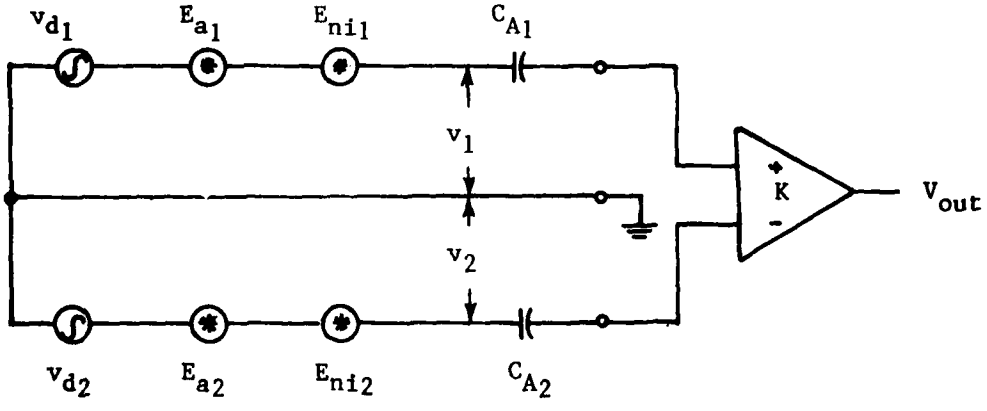

FIGURE 6. EQUIVALENT CIRCUIT - SIGNAL AND NOISE REFERRED TO INPUT

[4] H. H. Meinke, "Electrically Small Active Receiving Antennas," Proceedings, Ecom-Aro Workshop on Electrically Small Antennas, Fort Monmouth, New Jersey, May 6-7, 1976, pp. 35-41.

As before V_{d_1}, and V_{d_2} are the induced signal voltages from each half of the dipole. E_{a_1}, and E_{a_2} are the induced voltages (rms) due to the atmospheric noise field and E_{ni_1}, and E_{ni_2} are the equivalent input noise voltages (rms) due to self noise of the system. The active part of the system (including the noise blanker to be described later) is represented by a noiseless differential amplifier with system voltage gain K where $V_{out} = K(V_1 - V_2)$. Note that the system gain K includes the voltage drops across C_{A_1} and C_{A_2}. A clearer illustration of the signal-to-noise performance results when the balanced source and differential input system are replaced by an equivalent unbalanced source and single-ended input system. The signal voltages V_{d_1} and V_{d_2} are produced by the vertical electric field E_z in opposite halves of the dipole so $V_{d_2} = -V_{d_1}$. The noise voltages E_{a_1} and E_{a_2} although random produced by the same electric field and are therefore completely correlated ($c = -1$ or $E_{a_2}(t) = -E_{a_1}(t)$). The equivalent input noise sources are not correlated ($c = 0$) and therefore E_{ni_1}, and E_{ni_2} must be subtracted in the mean square sense. The resulting equivalent circuit is shown in Figure 7.

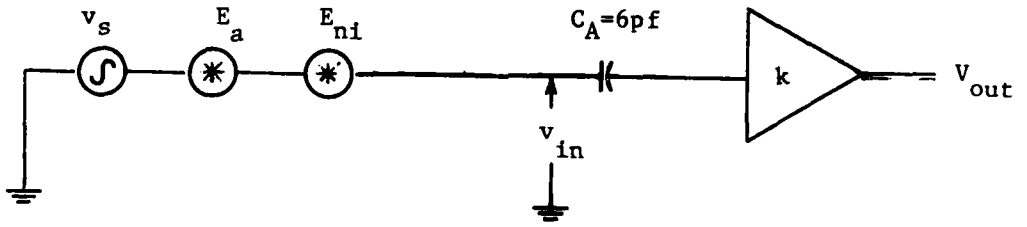

FIGURE 7. EQUIVALENT CIRCUIT (UNBALANCED)

The source values (rms) are as follows:

$$V_s = 0.05\ E_{zs}$$

$$E_a = 0.05\ E_{zn} \triangleq 0.3\text{nV/m}/\sqrt{\text{Hz}} \text{ @ } 1.66 \text{ MHz.}$$

$$E_{ni} = \sqrt{2}\ E_{ni_1} \triangleq 8.2\text{nV}/\sqrt{\text{Hz}} \text{ @ } 1.66 \text{ HMz.}$$

and the measured system voltage gain is

$$k = \frac{V_{out}}{V_{in}} \triangleq 0.9 \text{ @ } 1.66 \text{ MHz}$$

where $\triangleq$ indicates measured values for the system and $\triangleq$ indicates a typical value.[5] E_{zs} and E_{zn} are the rms values of the vertical electric field components of the signal and atmospheric noise fields, respectively. The E_{ni} source dominates and so the signal to noise ratio is given by

$$\frac{S}{N} = \frac{(0.05\ E_{zs})^2}{(\sqrt{2}\ E_{ni_1})^2 B_n} = \frac{(2.5 \times 10^{-3})\ E_{zs}^2}{(E_{ni}^2)(B_n)} = (3.72 \times 10^{13})\ \frac{E_{zs}^2}{B_n}$$

where B_n is the equivalent noise bandwidth in hertz of the total system including the receiver used with the antenna-noise blanker system. For example, if E_{zs} = 16.4 microvolts per metre and B_n is 1000 hertz, a signal-to-noise ratio of 10 (10 dB) should result. This is demonstrated in Figure 8. An input signal V_s = 0.82 microvolt rms (equivalent to 16.4 μV/m) at 1.66 MHz was connected to the preamplifier through an antenna equivalent circuit and the output of the system was amplified by a post amplifier with 49 dB gain. The lower trace in Figure 8 is the noise of the post amplifier alone. The upper trace is the post amplifier output when driven by the antenna-noise blanker system and shows the 10-dB signal-to-noise ratio.

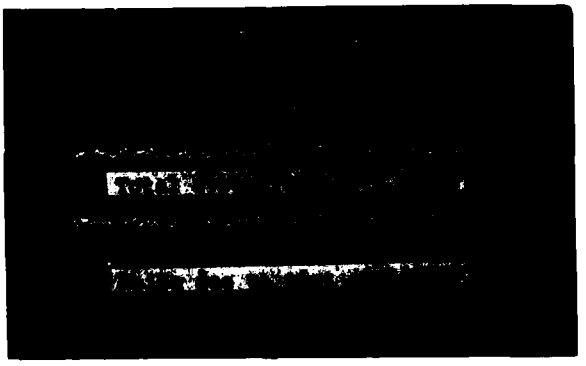

FIGURE 8. SIGNAL-TO-NOISE RATIO

[5]"World Distribution and Characteristics of Atmospheric Radio Noise," Int. Telecommunications Union, Geneva, Switzerland, Report 322, 1964.

Input Impedance

Since the small antenna capacitance C_A appears in series with the signal source V_s, it is important that the preamplifier input impedance be high to prevent excessive signal drop across C_A. The measured input impedance of the preamplifier at the frequencies of interest is essentially reactive and results from an input capacitance of about 5 picofarads. The resulting loss, which reduces the gain by a factor of 0.53, is included in the system voltage gain $k \stackrel{m}{=} 0.9$.

Common Mode Signal Rejection

The measured common mode voltage gain of the system is 2.82×10^{-3} at 3.3 MHz. The common mode input signal (atmospheric noise is negligible) from Figure 5 is $V_{cm} = 0.2\ E_{zs}$. Therefore the system output due to common mode signals is

$$V_o(cm) = (2.82 \times 10^{-3})\ (0.2)\ E_{zs} = (5.64 \times 10^{-4})\ E_{zs}.$$

The system output due to differential signals (assuming the desired signal is much larger than the self-noise of the system) is

$$V_o\ (diff) = k\ (0.05\ E_{zs}) = 0.045\ E_{zs}.$$

Therefore, at the system output the common mode signals are about 38 dB below the desired differential signals.

Linearity

Nonlinearities in the gain of the antenna-noise blanker system can cause the generation of unwanted signals that fall within the frequency range of the desired Raydist signals. A typical Raydist net operates on the following frequencies simultaneously:

f_1 = 1.654647 MHz (red sideband)

f_2 = 1.655017 MHz (red carrier)

f_3 = 1.655422 MHz (green sideband)

f_4 = 1.655722 MHz (green carrier)

f_5 = 3.310404 MHz (red cw)

f_6 = 3.310554 MHz (green cw).

A second order nonlinearity will cause unwanted signals to appear at frequencies given by $2f_i$, $2f_j$, and $f_i \pm f_j$ ($i = 1,2,\ldots,6$ $j = 1,2,\ldots,6$). One such second order intermodulation product is $f_1 + f_4 = 3.310419$ MHz which differs from f_5 by only 14 hertz. A third order nonlinearity is especially troublesome since it causes unwanted signals to appear at frequencies given by $3f_i$, $3f_j$, $2f_i \pm f_j$ and $f_i \pm 2f_j$. The intermodulation products can occur at frequencies close to the desired signals which produced them. One such condition is the third order intermodulation product $2f_2 - f_1 = 1.655387$ MHz which differs from f_3 by only 55 hertz. A third order nonlinearity also allows a modulated interfering signal to cross modulate a desired signal.

Measurements of the input signal level required to produce one decibel of gain compression due to nonlinearity, and the second and third order intercept points (extrapolated input levels which produce intermodulation products and signals of equal amplitudes) for the antenna-noise blanker system resulted in the following data after conversion of the input signal voltages to equivalent vertical electric field intensities:

1. One dB compression point: $E_z = 7.1$ volts/metre at 1.66 MHz.
2. Second order intercept point: $E_z = 106$ volts/metre ($f_1 = 1.660$ MHz, $f_2 = 1.662$ MHz, equal levels)
3. Third order intercept point: $E_z = 37.7$ volts/metre (f_1, f_2 same as 2 above).

Cross modulation of a 1.66 MHz signal by an interfering amplitude modulated (30 percent - 400 Hz) signal was measured by finding the level of the interfering signal required to produce 3 percent amplitude modulation of the 1.66 MHz signal. These levels in equivalent electric field intensity versus frequency are shown in Figure 9.

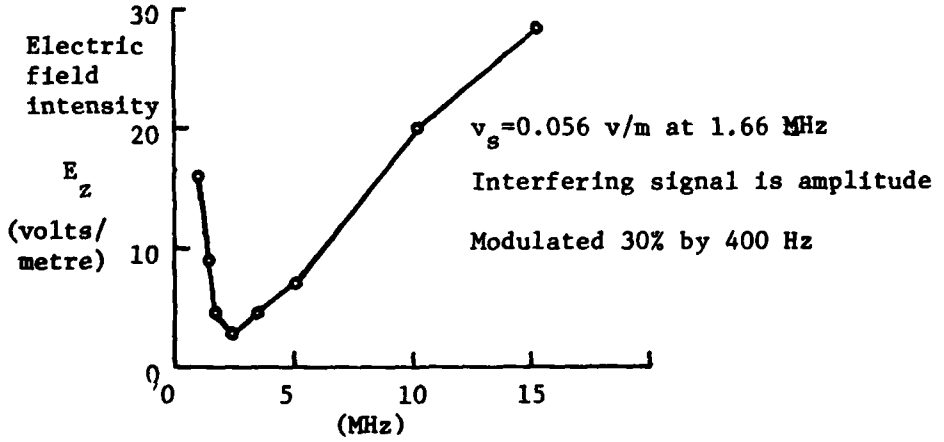

FIGURE 9. CROSS MODULATION PERFORMANCE

Preamplifier Circuit Description

The active dipole antenna preamplifier is shown schematically in Figure 10. The balanced input stage uses a Siliconix type U440 matched dual N-channel junction field effect transistor (NJFET) (Q_1) as a differential amplifier. The antenna elements operate at ground potential and are ac coupled to the transistor gates which are biased at about 8 volts dc. A balance control (R_8) allows the preamplifier to be adjusted for maximum rejection of common mode signals. The differential output of Q_1 is transformed to a single ended drive signal for Q_2 by tuned transformer T_1. The primary and secondary of T_1 consist of bifilar windings of six and eight turns, respectively, on a ferrite toroidal core (Ferroxcube 768T188-3D3). The primary is connected to form a 12-turn center tapped winding while the secondary is connected to form a single 16-turn winding. This construction technique preserves the balance of the differential amplifier by equalizing the capacitive loading on the opposite ends of the primary. The transformer secondary is tuned to resonate at the geometric mean frequency of the lowest and highest frequencies of interest (f_o = 2.34 MHz) by C_5 and the already low Q is further reduced to about 1.4 by the loading of resistor R_9 to provide a 3 dB bandwidth of 1.65 MHz to 3.31 MHz. The voltage gain of -2 (at f_o) at the drain terminals of Q_1 results in a maximum input capacitance due to Miller effect of

$$C_{IN(MAX)} = C_{gs(MAX)} + (1-A)\, C_{gd(MAX)} + C_{STRAY} = 3.5 + (3)(0.8)$$

$$+ C_{STRAY} = 5.9 + C_{STRAY} \text{ (pf)} .$$

Measured values of input capacitance average about 5.3 picofarads. The input capacitance is, therefore, about the same as the effective antenna capacitance while a differential voltage gain of about -2.8 is obtained in the first stage measured at the output of T_1.

The second stage uses a Siliconix U310 NJFET connected in the common source configuration. The output is transformer-coupled via T_2 to the transmission line. T_2 is a broad band transmission line transformer consisting of four trifilar turns on a ferrite toroidal core (Ferroxcube T768-188-3E2A) and connected as a 3-to-1 turns ratio autotransformer. The parallel combination of R_{11} and the output impedance of Q_2 is stepped down to provide a 50-ohm output impedance. T_2 also serves to decouple the dc power supply and RF signal circuits to allow both power and signal to be carried by a single coaxial cable. The net voltage gain from the gate of Q_2 to the output connector is slightly greater than 1, making the total differential voltage gain at 2.34 MHz about 3. The signal voltage drop across the antenna capacitance due to preamplifier input capacitance reduces the gain by a factor of 0.53.

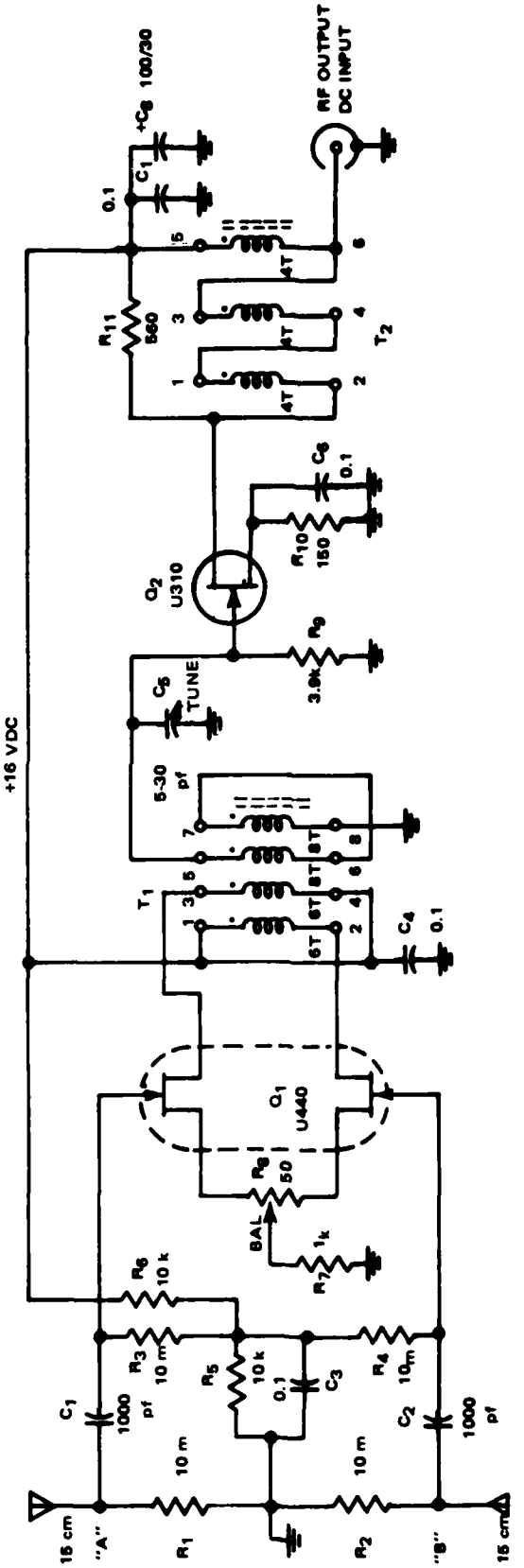

FIGURE 10. ACTIVE DIPOLE ANTENNA PREAMPLIFIER

Therefore, the total differential system gain is about 1.6 at 2.34 MHz decreasing to 1.1 at 1.65 and 3.31 MHz. At the Raydist frequencies the output voltage of the antenna-preamplifier is given by

$$V_o = 1.1\ (0.05\ E_{zs}) = 0.055\ E_{zs}$$

across a 50-ohm load.

NOISE BLANKER DEVELOPMENT

INTRODUCTION

The cause of the impulse noise which degrades Raydist performance aboard AMCM helicopters was identified by McDonnell Douglas Research Laboratories personnel as negative-corona discharge from the tow cable end. The noise consists of pulses (Trichel pulses) with distinct temporal and spectral characteristics.[6] The Trichel pulse has a very short rise time of less than 10 nanoseconds, and exponential decay, and a duration of from 0.01 to 5 microseconds. The spectral density is essentially constant over the band of frequencies used by Raydist. In order to facilitate the development and testing of the noise blanker, a test pulse generator was constructed to provide pulses with Trichel pulse characteristics. The test generator shown schematically in Figure 11 is a relaxation oscillator using an NPN silicon switching transistor in the avalanche breakdown mode. The generator outputs about 1 volt across a 50-ohm load as shown in Figure 12a. Figure 12b shows the spectral content from 0 to 20 MHz measured in a 100-kHz bandwidth. A -20 dBm 10-MHz signal was added for reference. Use of the test generator is of course simpler, safer, and more repeatable than actual high voltage corona generator techniques.

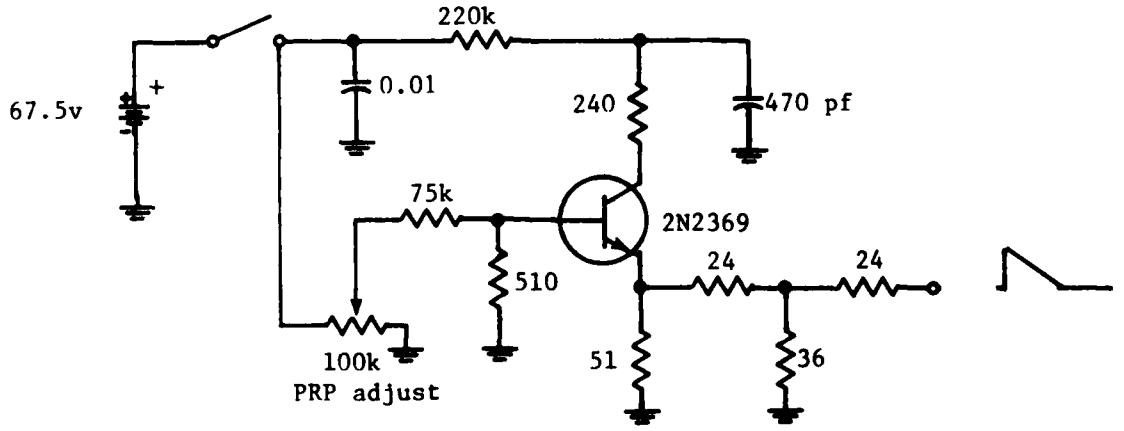

FIGURE 11. TEST PULSE GENERATOR SCHEMATIC

[6]Shaffer, J. F. and Peng, T. C., "High Potential Clouds in Jet Engine Exhaust," Journal of the AIAA, Vol. 15, No. 3, 1977.

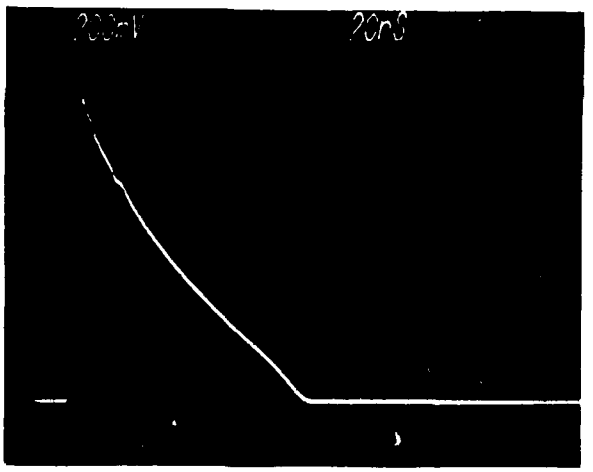

a. Pulse waveform across 50 ohm load

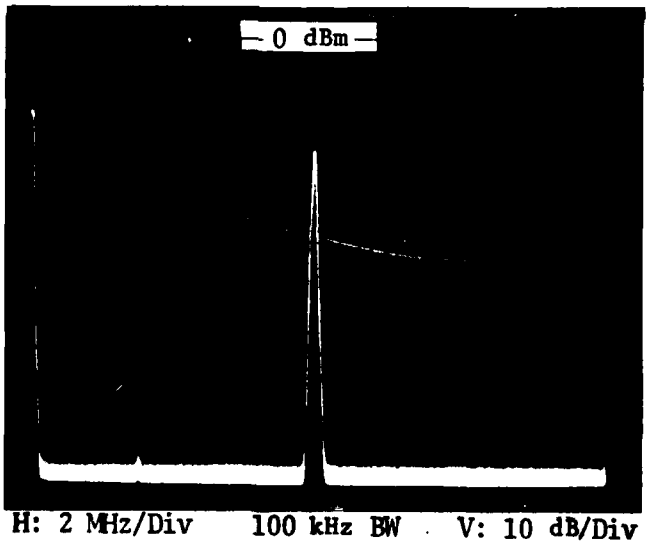

b. Pulse spectrum (100 kHz bandwidth)

FIGURE 12. TEST GENERATOR PULSE CHARACTERISTICS

Trichel pulse noise degrades Raydist performance in two ways. The pulses are generally of large amplitude relative to the desired signals and may drive the receiver circuits into nonlinear operating regions (overload). Also the wide bandwidth pulses have significant energy content in frequency components that are within the passbands of the narrow bandwidth receiver circuits. This energy propagates through those circuits and emerges in the form of sinusoidal oscillations with an envelope having relatively slow rise and fall times. These noise-produced oscillations are essentially indistinguishable from the desired signals and cause considerable interference. Therefore, the noise pulses must be eliminated before they are modified by passage through a narrow bandwidth circuit. The antenna input circuit of the Raydist receiver is a bandpass filter with a bandwidth of about 30 kHz.[7] So elimination of the Trichel pulse noise is best done before it enters the receiver. External processing is also in keeping with the desire to not require internal modification of the receiver.

Impulsive noise in radio receivers is generally suppressed in one of two ways. Amplitude limiters or clippers limit the maximum amplitude of the noise pulse to about the level of the desired signals. Noise blankers suppress the noise by reducing the gain of the signal path to a low value in the presence of a noise pulse.[8] The presence of a noise pulse in either technique is indicated when the signal-plus-noise exceeds an amplitude threshold. Suppression of the noise pulses external to the receiver, i.e., in the circuit between the antenna and the receiver input, requires processing desired signals with voltage levels ranging from about 2 microvolts to about 20 millivolts and noise pulses with voltage levels ranging from a few millivolts to more than 1 volt. Consideration of the hardware and techniques available to do the processing required by the two suppression techniques on such signal and noise pulse levels led to use of the noise blanker method.

The basic components required by the noise blanker are shown in Figure 13.

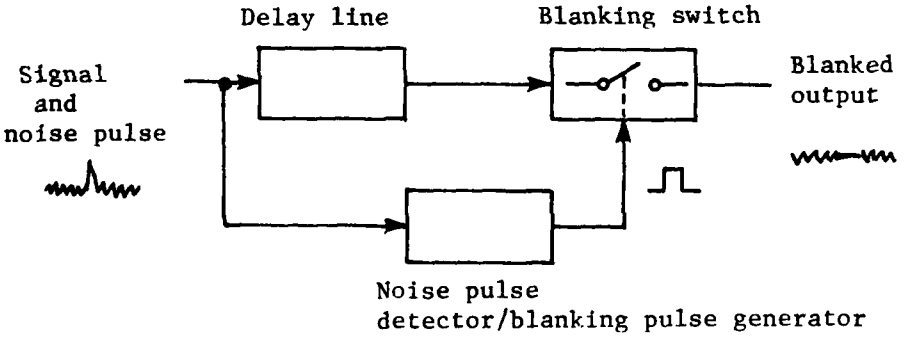

FIGURE 13. BASIC IMPULSE NOISE BLANKER

[7]Teledyne Hastings - Raydist Instruction Manual, "Raydist Range Navigation Receiver Model RA-89, MR-194, 26 August 1980.

[8]Gosling, W., "Impulsive Noise Reduction in Radio Receivers," The Radio and Electronic Engineer, Vol. 43, No. 5, May 1973, p. 341.

The delay line simply delays the noise pulse sufficiently to allow for the non-zero response time of the noise pulse detector-blanking pulse generator and blanking switch. The blanking switch is the most critical component. It must provide a relatively small insertion loss when closed, a large insertion loss when open, and it must be able to rapidly switch from one state to the other without coupling switching command signal transients into the RF signal path. Such switching transients would themselves be impulsive-type noise. Also, it must have sufficient bandwidth and must be compatible with the voltage levels and impedance of the rest of the circuit. The double balanced Schottky diode mixer (DBM) meets these requirements and at the same time is inexpensive and reliable.

The complete noise blanker system shown in Figure 14 is inserted in series with the 50-ohm coaxial cable between the active dipole antenna and the Raydist receiver antenna input.

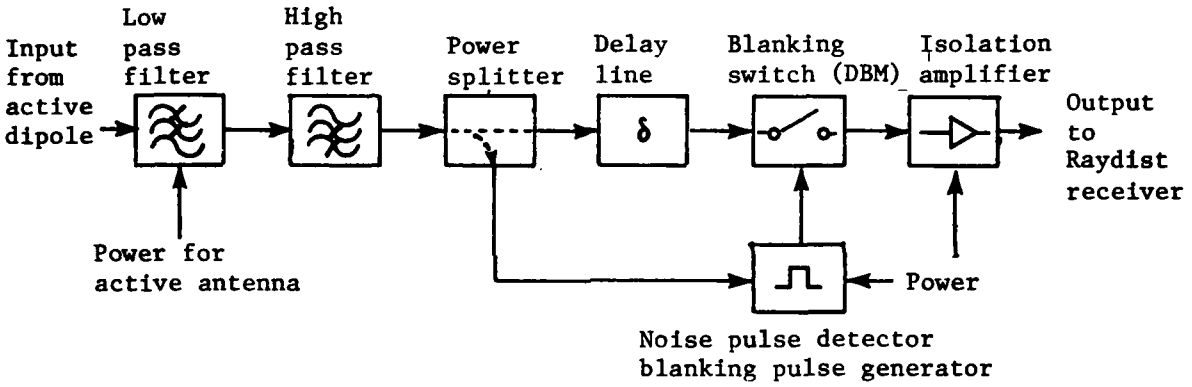

FIGURE 14. NOISE BLANKER SYSTEM

All the circuit blocks in Figure 14 have 50-ohm input and output impedances are interconnected by 50-ohm coaxial cables. The circuit blocks shown in Figure 14 that are not included in the basic noise blanker are described below.

Neither noise pulses nor desired signals reach the receiver when the blanking switch is open. To prevent excessive loss of desired signals as a result of high rate triggering of the noise pulse detector the minimum retrigger time of the blanking pulse generator is set to three times the blanking pulse duration (10 microseconds of blanked output every 30 microseconds). In the presence of a high level periodic signal such as might be produced by a nearby AM broadcast station or transmitting equipment on board the helicopter, maximum rate triggering on that signal could make the noise blanker unable to respond to noise pulses. Therefore, it is desirable to band limit the noise blanker input signals. However, sufficient bandwidth must be maintained to preclude significant distortion of the noise pulses as discussed above. The low pass and high pass filters shown in Figure 14 form a bandpass network which attenuates inputs with frequencies above 5.5 MHz and below 1.5 MHz.

The power splitter shown in Figure 14 is a two-way 0-degree hybrid transformer which divides the signal path into two equal channels while maintaining the proper impedance matching.

The output impedance of the blanking switch is 50 ohms when it is closed and is a high value when the switch is open. If this changing source impedance were connected directly to the Raydist receiver antenna input, it would modulate the first local oscillator leakage from the receiver and thereby produce interfering sideband frequencies. The isolation amplifier shown in Figure 14 prevents this problem by providing a constant 50-ohm output impedance and a high degree of reverse isolation.

The operation of the noise blanker system is shown in Figures 15 and 16. Figure 15 shows the voltage waveforms associated with the response to a single noise pulse with the blanker disabled and with the blanker in operation. In Figure 15b the blanker switch is seen to be completely open at about 300 nanoseconds after the leading edge of the noise pulse or about 200 nanoseconds before the pulse exits the 500-nanosecond delay line. The sequence of photographs in Figure 16 shows the frequency spectrum of the output of the entire system (including the active dipole antenna) with Raydist signals only present (Figure 16a), signals and noise pulses present with the blanker off (Figure 16b), and signals and noise present with the blanker on (Figure 16c). The signals are typical Raydist signals at 1.65 MHz and 3.31 MHz with power levels of -50 dBm. Figure 16b shows the approximate frequency response of the antenna preamplifier and low pass and high pass filters. The noise shown produced frequent "lane jump" errors in the phase indicator readings of a Raydist T receiving system (ZA-75C-1/GA-62). Figure 16c shows complete elimination of the trichel pulse noise. The residual switching transient noise visible just above the spectrum analyzer noise floor produced no response in the Raydist system, but blanking of the Trichel pulse noise restored normal operation.

NOISE BLANKER SYSTEM CIRCUIT DESCRIPTION

Low-Pass Filter

The low-pass filter shown schematically in Figure 17 is a fifth-order Chebyshev Type with 0.01 dB passband ripple and a cutoff frequency (-3 dB) of 5.5 MHz. The filter attenuation increases at a 30 dB per octave rate above cutoff. The dc power supply for the active dipole preamplifier is connected to the low-pass filter RF signal path through a decoupling network (R_1, C_4, $L3$).

High-Pass Filter

The high-pass filter shown schematically in Figure 18a is a high-pass transformation of a seventh order Chebyshev-Cauer (Elliptic) low-pass type with a passband reflection coefficient of 5 percent, a modular angle of

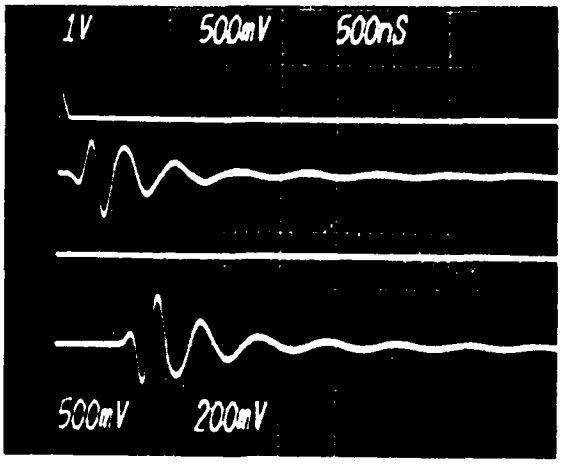

a. Noise blanker off

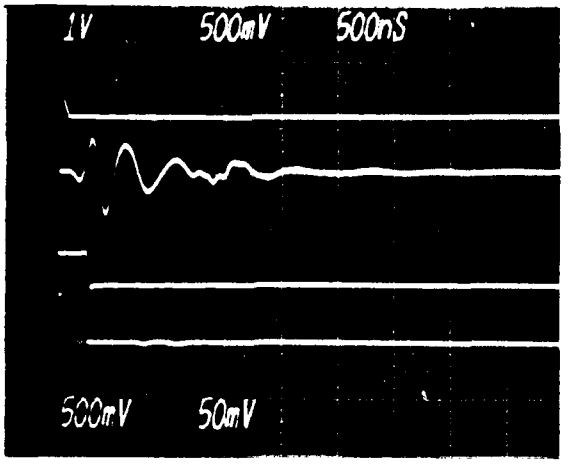

b. Noise blanker on

1. (Top waveform) noise pulse at input
2. Input to delay line
3. Blanking pulse (low level blanks)
4. (Bottom waveform) system output

FIGURE 15. NOISE BLANKER SYSTEM WAVEFORMS

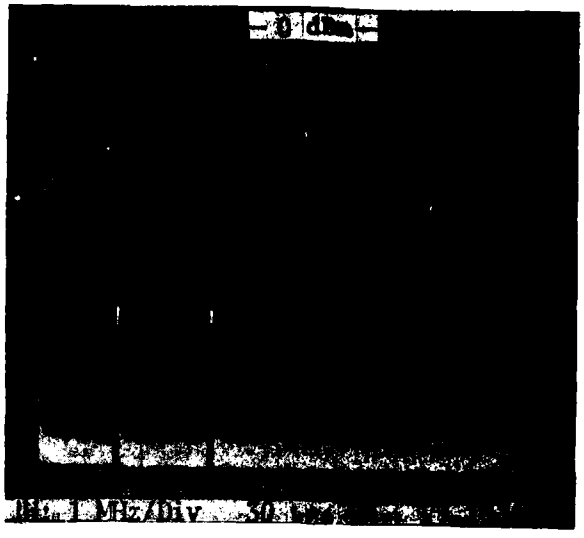

a. Raydist signals only (-50 dBm at 1.65 MHz and 3.31 MHz)

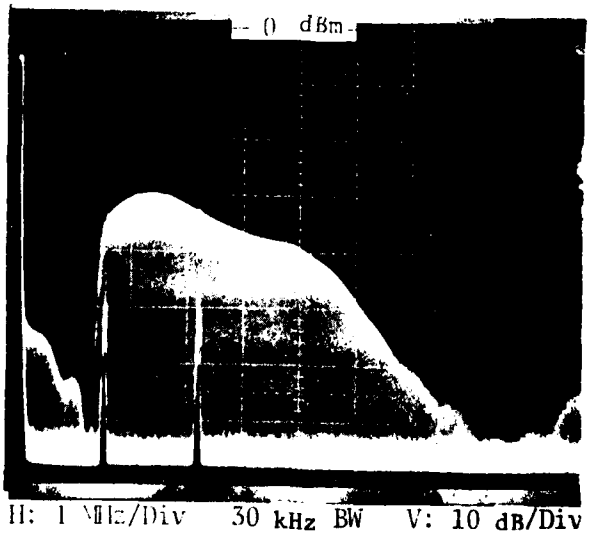

b. Raydist signals and trichel pulse noise blanker off

FIGURE 16. SYSTEM OUTPUT FREQUENCY SPECTRUM

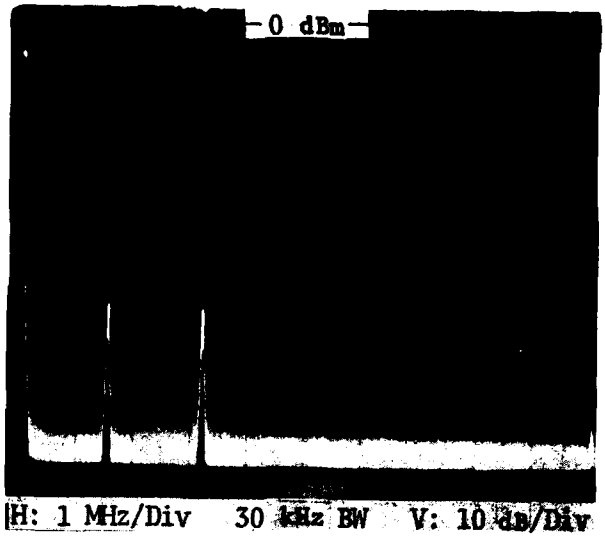

c. Raydist signals and trichel pulse noise blanker on

FIGURE 16. SYSTEM OUTPUT FREQUENCY SPECTRUM

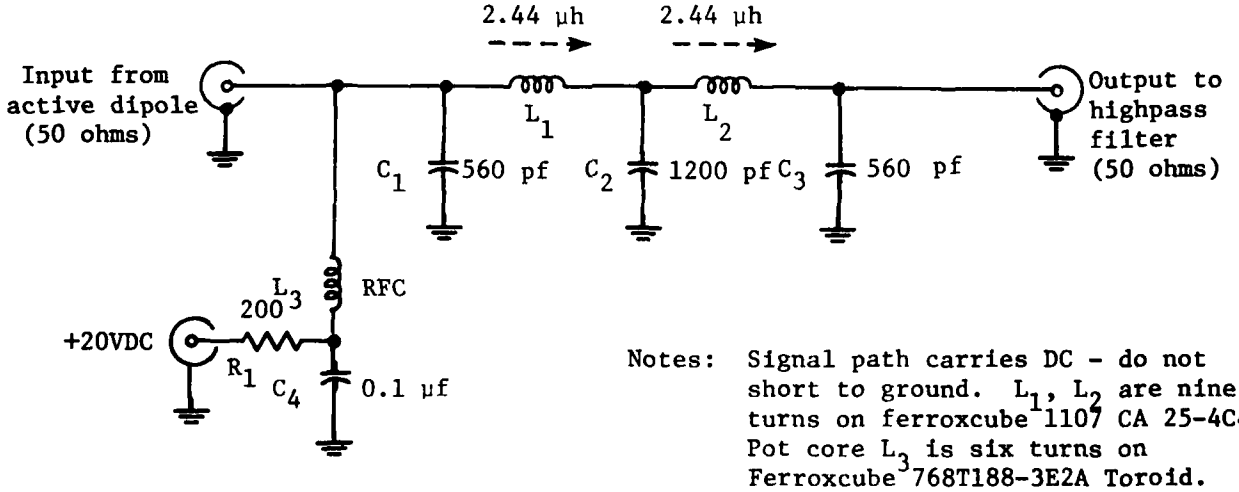

Notes: Signal path carries DC - do not short to ground. L_1, L_2 are nine turns on ferroxcube 1107 CA 25-4C4. Pot core L_3 is six turns on Ferroxcube 768T188-3E2A Toroid.

FIGURE 17. LOW-PASS FILTER (CHEBYSHEV, N=5, PASSBAND RIPPLE= 0.01 dB, f_c = 5.5 MHz)

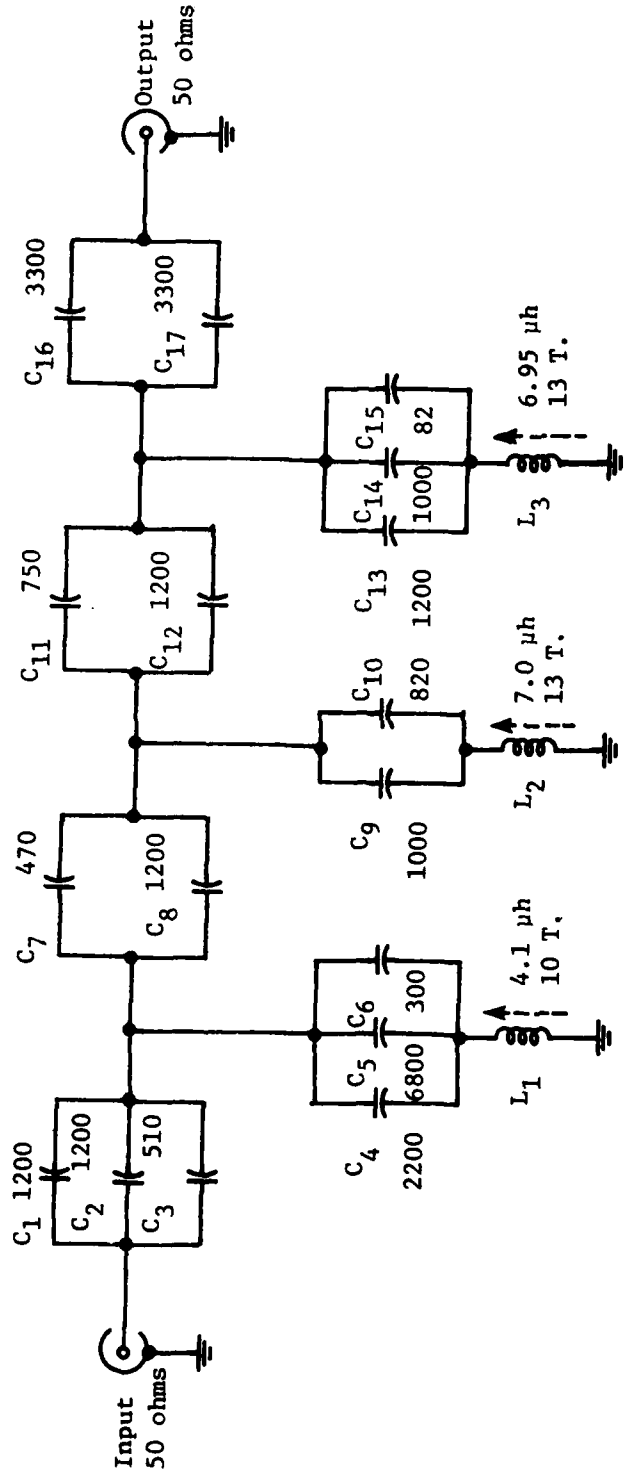

Notes: All capacitance values are PF.
All inductors wound on Ferroxcube 1107CA 40-4C4 pot cores

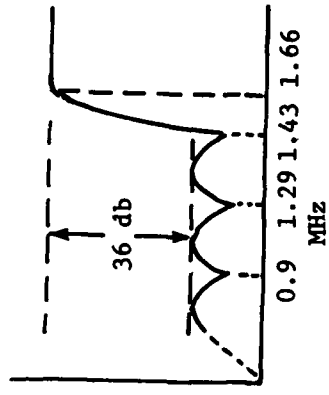

FIGURE 18. HIGH-PASS FILTER SCHEMATIC AND FREQUENCY RESPONSE

60 degrees, and equal termination impedances of 50 ohms.[9] The 0.01-dB cutoff frequency is about 1.67 MHz. The filter provides a minimum attenuation of about 36 dB below about 1.45 MHz as shown in Figure 18b and also blocks the dc voltage present at the output of the low-pass filter.

Power Splitter, Delay Line, and Blanking Switch

The power splitter, delay line, and blanking switch are shown in Figure 19. The power splitter manufactured by Mini-Circuits, Inc., is a two-way 0-degree hybrid transformer. Power input to the sum port (S) is divided equally between ports 1 and 2. The impedance at all ports is 50 ohms. The delay line manufactured by Allen Avionics, Inc., has a delay of 500 nanoseconds, a -3 dB bandwidth of 12 MHz, and 50-ohm port impedances. The blanking switch is a double balanced Schottky diode mixer (DBM) also manufactured by Mini-Circuits, Inc. Due to the circuit symmetry of the DBM a high degree of isolation exists between the R and L ports when no signal is applied to the I port. A current into the I port upsets the balance and couples the R and L ports. Also because of the circuit symmetry, switching currents into the I Port are isolated from the signal path (R and L ports). The external balance network (R_1 - R_3, C_1) was added to the DBM to allow precise adjustment of the balance in order to obtain minimal switching transient noise.

Noise Pulse Detector and Blanking Pulse Generator

The noise pulse detector/blanking pulse generator is shown schematically in Figure 20. Dual comparator U_1 forms a window detector centered on 0 volts with equal magnitude thresholds set by R_8. This provides minimum detection delay independent of input noise pulse polarity. Transformer T_1 multiplies the input voltage level by three and transformer T_2 drives the comparator inputs with equal amplitude opposite phase voltages. This allows using a single reference voltage for upper and lower threshold.

The comparator outputs are logically combined in an OR gate formed by Schottky diodes D_1 and D_2 and resistor R_5. The OR gate is used rather than a "wired AND" connection of the open collector comparator outputs since the LM319 integrated circuit has a shorter response time to an input which produces a positive going output. The voltage convertor integrated circuit U_3 provides a negative supply and reference voltage which allows the signal inputs of the comparators to be biased at 0 volts. The voltage regulator integrated circuit provides a constant +5 volt supply. When the input noise pulse does not exceed the positive or negative threshold, the one-shot multivibrator U_4A is not triggered and VMOS transistor Q_1 is off. A

---

[9]Zverev, Anatol I., "Handbook of Filter Synthesis," Joan Wiley and Sons, Inc., 1967, p. 268.

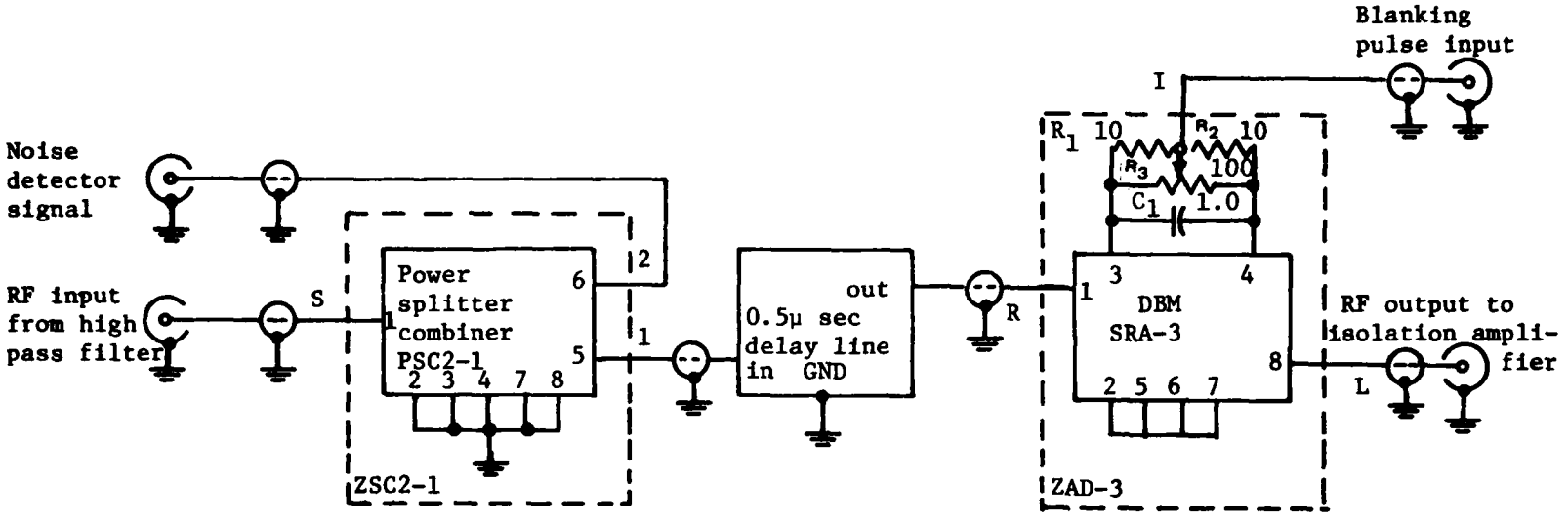

Power splitter/combiner: Mini-circuits lab2-way 0° TYPE ZSC2-1 (or PSC2-1 for PC board)
Delay line: Allen Avionics TYPE SP0500Z050 0.5 μsec Z = 50 Ω.
Doubly balanced mixer: Mini-circuits lab TYPE ZAD-3 (modified by addition of RC network to SRA-3 inside case) or SRA-3 and RC network for PC board.

Note: Original systems used ZSC2-1 and ZAD-3 models (packaged versions with BNC connectors interconnected by 50-Ω coaxial cables). The RC balance network was installed on the SRA-3 mixer inside the ZAD-3 case. It is recommended that new systems use the PSC 2-1 and SRA-3 along with the delay line and RC network all mounted on a printed circuit board. Adjustment of the balance network is for minimal switching transient noise.

FIGURE 19. POWER SPLITTER/DELAY LINE/BLANKING SWITCH

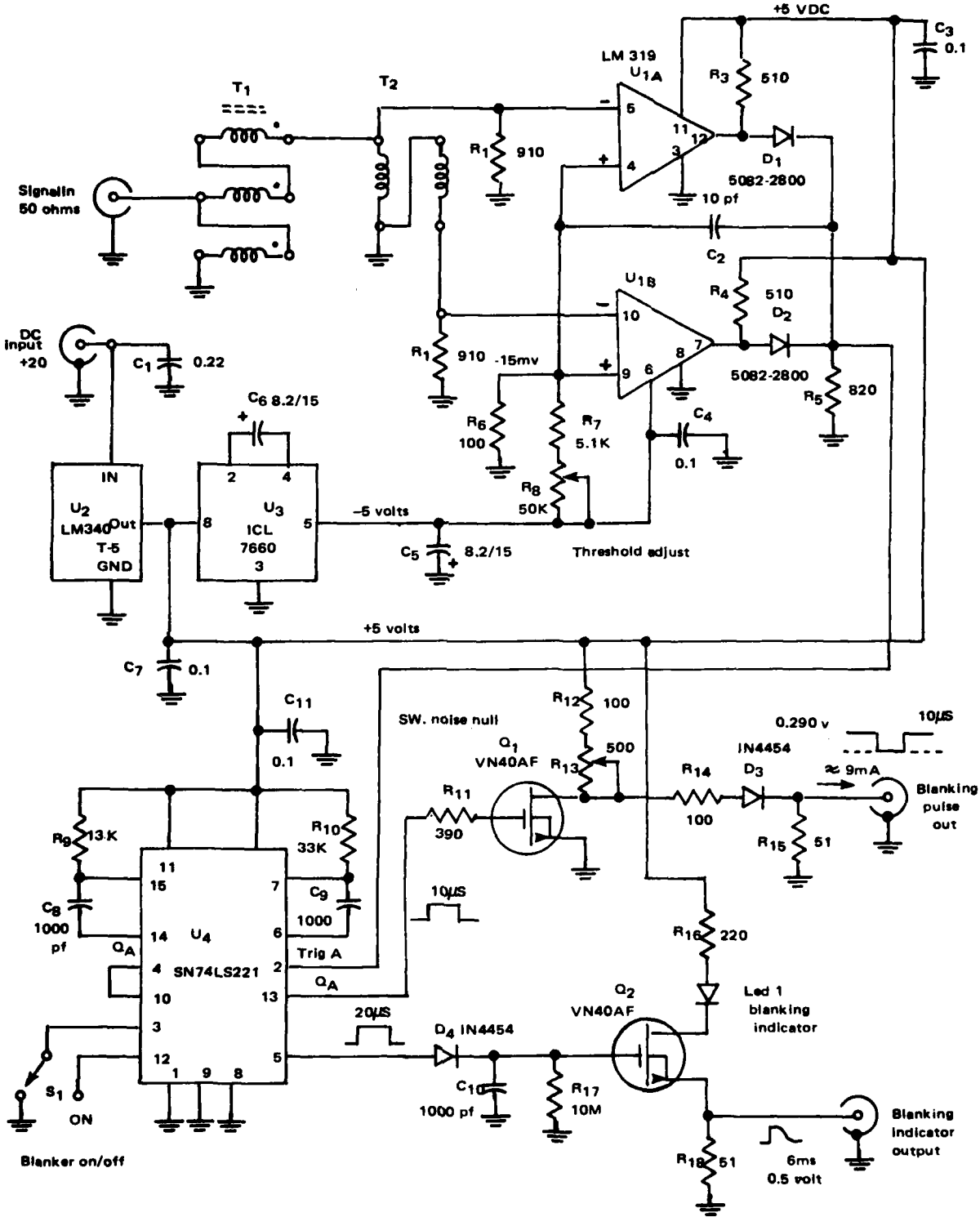

FIGURE 20. NOISE PULSE DETECTOR/BLANKING PULSE GENERATOR

portion of the current flowing from the +5 volt supply through resistors R_{12}, R_{13}, and R_{14}, and diode D_3 enters the I port of the DBM, thus closing the blanking switch. When either a positive or negative noise pulse exceeds its respective threshold, the positive-going output of the OR gate triggers the one-shot multivibrator U_4A. The 10-microsecond pulse from U_4A turns VMOS transistor Q_1 on, thus shunting the current flowing through R_{12} and R_{13} to ground. The current into the I port of the DBM goes to zero and the blanking switch opens for 10 microseconds. The trailing edge of the pulse from U_4A triggers one-shot multivibration U_4B which outputs a 20-microsecond pulse which holds U_4A in a reset state. This limits the maximum blanking rate to 10 microseconds of blanking every 30 microseconds. The 20-microsecond pulse is stretched in the peak detector circuit which drives VMOS transistor Q_2. When a blanking pulse is generated, Q_2 activates the light emitting diode blanking indicator and outputs a blanking indicator pulse for remote display purposes. Resistor R_{13} sets the quiescent current into the DBM I port when the blanking switch is closed. Resistor R_{13} and the DBM balance control R_3 (Figure 19) are adjusted to minimize the switching transients generates when the blanking switch opens.

Isolation Amplifier

The isolation amplifier is shown schematically in Figure 21. It uses a Siliconix U310 NJFET in the common source configuration. R_1 sets the input impedance to near 50 ohms. Transformer T_1, a quadrifilar-wound transmission line transformer, steps the output impedance of Q_1 in parallel with R_3 down to about 50 ohms. The forward gain is 4 dB while the reverse gain (isolation) is about -55 dB at 1.6 MHz and about -50 dB at 3.3 MHz. The forward gain partially compensates for the loss of gain in the DBM (blanking switch). Good impedance matching is provided to the DBM and Raydist receiver and the receiver is effectively isolated from the changing output impedance of the DBM.

The 20-volt power supply is provided by either a 115-volt 400-Hz to 20 volt dc regulated supply or an integrated circuit voltage regulator operating from the helicopter's 28-volt dc supply.

CONCLUSIONS

The balanced active antenna and impulse noise blanker system described herein have provided a significant improvement in the operation of the Raydist T radio navigation system aboard AMCM helicopters. Laboratory test

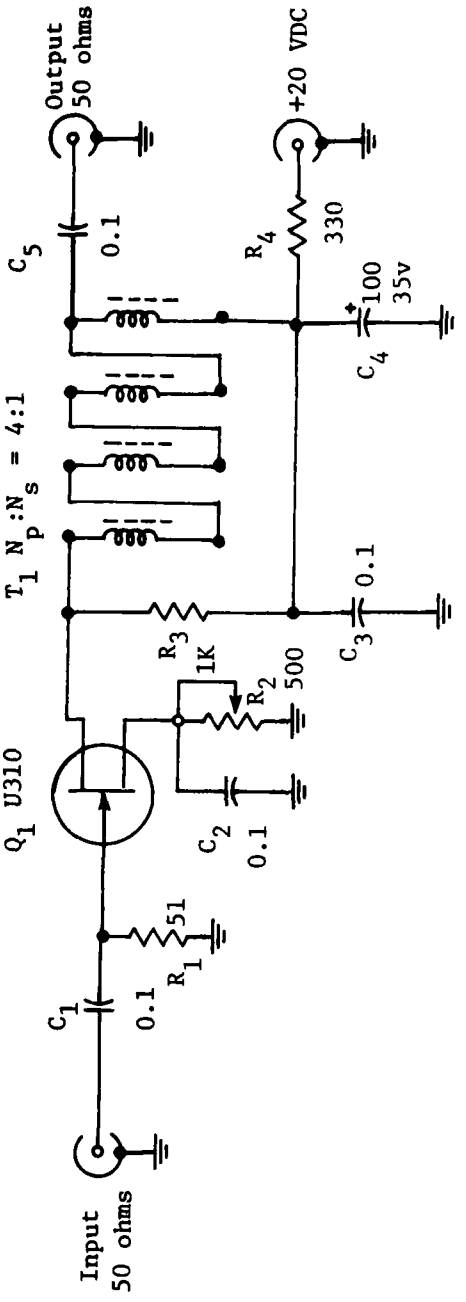

Notes: 1. Adjust R_2 for I_D = 15 MA

2. T_1 is 4 quadrifilar turns of #30 wire on ferroxcube 768T188-3E2A toroid

FIGURE 21. ISOLATION AMPLIFIER

results have been described and the results of field test operations have been reported in Eisenhauer's letter report. The system is easily added to the Raydist equipment by simply connecting to the aircraft power supply and to the Raydist receiver antenna input connector. The antenna provides the Raydist receiver with normal level signals in the range of from -100 dBm to -20 dBm in the presence of vertical electric field intensities of from 50 microvolts/metre to about 500 millivolts/metre. The noise blanker is effective in suppressing impulse noise with pulse durations of less than 10 microseconds and pulse repetition periods greater than 30 microseconds. The system linearity and dynamic range have proved adequate but could be improved by suitable redesign should the need arise.

DISTRIBUTION LIST

		Copy No.
162	Commander, Naval Air Systems Command, Naval Air Systems Command Headquarters, Washington, DC 20361 (AIR 548)	1-4
427	Commander, Naval Sea Systems Command, Naval Sea Systems Command Headquarters, Washington, DC 20362 (NAVSEA 63R)	5
	(NAVSEA PMS 407)	6
	(NAVSEA 63Z3)	7
396	Commander, Naval Air Force, Atlantic Fleet, Naval Air Station, Norfolk, VA 23511	8
479	Commander, Naval Surface Force, US Atlantic Fleet, Norfolk, VA 23511	9
146	Commander, Mine Warfare Command, Naval Base, Charleston, SC 29408	10
---	Commander, Mine Squadron FIVE, Naval Support Activity, Seattle, Washington, 98115	11
---	Commander, Mine Squadron TWELVE, FPO, New York 09501	12
368	Commanding Officer, Helicopter Mine Squadron TWELVE (HM-12), Naval Air Station, Norfolk, VA 23511	13
---	Commanding Officer, Helicopter Mine Squadron FOURTEEN (HM-14), Naval Air Station, Norfolk, VA 23511	14
---	Commanding Officer, Helicopter Mine Squadron SIXTEEN (HM-16), Naval Air Station, Norfolk, VA 23511	15
075	Defense Technical Information Center	16-25

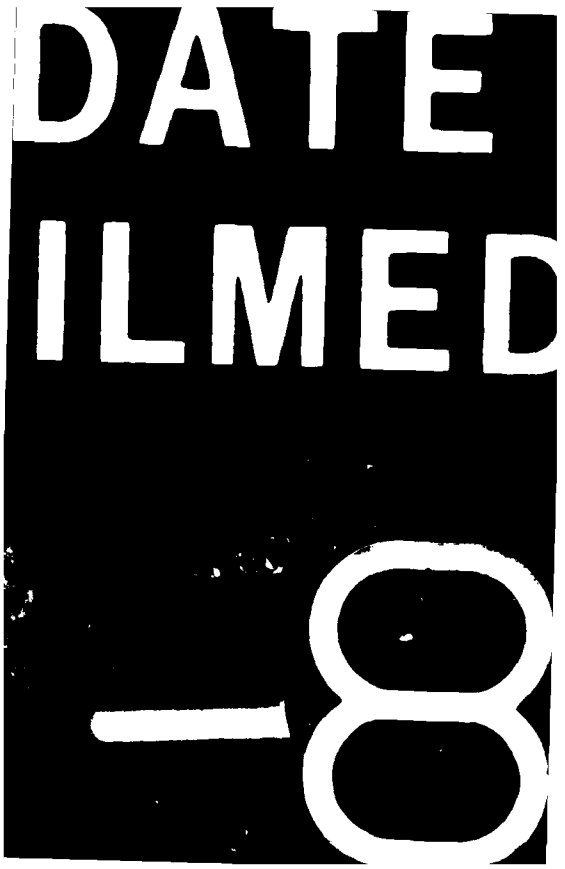
DATE
ILMED
-8